A New Modelling Approach for Turbulent Astrophysical Flows

J. C. Niemeyer, W. Schmidt, A. Maier, M. Hupp & Ch. Federrath

We present three-dimensional numerical simulations of supersonic isotropic turbulence in a periodic box subject to stochastic forcing. The finite-volume code Enzo from UCSD is utilised with the piece-wise-parabolic method [Colella and Woodward, 1984] to solve the compressible Euler equations. To begin with, a static grid of 768^3 *cells is used in combination with a Ornstein-Uhlenbeck-type driving force [Schmidt et al., 2006] that comprises predominantly compressive modes. The ideal gas equation is applied with* $\gamma = 1.4$ *(adiabatic) in one simulation and* $\gamma = 1.01$ *(nearly isothermal) in a second simulation. Analysing structural properties of the flow realizations, we intend to formulate appropriate criteria for the efficient application of adaptive mesh refinement (AMR) in astrophysical turbulence simulations.*

Stochastic Forcing

- In the simulations, fluid is stirred by a random force field that smoothly varies in space and time.
- The discrete Fourier modes of the acceleration $\hat{\boldsymbol{a}}_{jlm}(t)$ are determined by a Langevin-type stochastic differential equation (SDE):

$$\mathrm{d}\hat{\boldsymbol{a}}_{jlm}(t) = -\hat{\boldsymbol{a}}_{jlm}(t)\frac{\mathrm{d}t}{T} + F_0\left(\frac{2\sigma^2(\boldsymbol{k})}{T}\right)^{1/2} \boldsymbol{P}_\zeta(\boldsymbol{k}_{jlm})\cdot\mathrm{d}\boldsymbol{\mathcal{W}}_t.$$

  The second term generates Gaussian random deviates ($\boldsymbol{\mathcal{W}}_t$ is called the *Wiener process*). In one-dimensional form the above SDE describes the *Ornstein-Uhlenbeck process*.
- The spectrum of the force field is determined by $\sigma(\boldsymbol{k})$. We apply forcing on the largest length scales only. The corresponding characteristic wavenumber $k_0 = 2\pi\alpha/X$, where X is the size of the physical domain. There are non-zero modes for $|\boldsymbol{k}| \in [0, 2k_0]$. In the simulations presented here, $\alpha = 2$ (i. e., the forcing wavelength is about half of the domain size).
- The forcing is either solenoidal (divergence-free) or dilatational (rotation-free) or a weighted combination of both. This property of the force field is controlled by means of the projection operator

$$(P_{ij})_\zeta(\boldsymbol{k}) = \zeta P^\perp_{ij}(\boldsymbol{k}) + (1-\zeta)P^\parallel_{ij}(\boldsymbol{k}) = \zeta\delta_{ij} + (1-2\zeta)\frac{k_i k_j}{k^2}.$$

  For solenoidal modes, $\zeta = 1$ ($\boldsymbol{k}\cdot\hat{\boldsymbol{a}} = 0$), whereas $\zeta = 0$ ($\boldsymbol{k}\times\hat{\boldsymbol{a}} = 0$) for dilatational modes. We set $\zeta = 0.1$. Thus, compression dominates over rotation in our simulations.
- The autocorrelation time scale T determines the evolution of the force field. The memory of earlier flow configurations is damped exponentially over the time T. We identify T with the large-eddy turn-over time of the turbulent flow, i. e., $T = V/L$.
- The magnitude F_0 of the forcing modes is chosen such that $f_{\mathrm{rms}} = \sqrt{3}V/T$. Setting $V = 5c_0/\sqrt{3}$, the characteristic initial Mach number in our simulations equals 5.0.

Mass Density and Mach Number

- Global averages characterise the overall evolution of the system. Below, the root mean squares (RMS) of the normalised velocity v/V and the Mach number $\mathrm{Ma} = v/c_\mathrm{s}$ are plotted as functions of time for $\gamma = 1.4$. Initially, there is a steep rise due to the formation of shocks. The RMS velocity quickly adjusts to a statistically stationary state. The RMS Mach number, on the other hand, gradually decreases, because the heat produced by the dissipation of kinetic energy rises the speed of sound in camprison to the flow velocity.

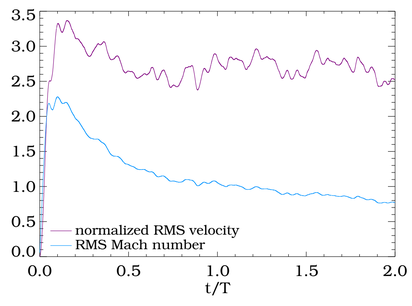

Figure 1: Evolution of the root mean square (RMS) velocity in units of V and the RMS Mach number, respectively, for $\gamma = 1.4$ (adiabatic equation of state).

- Probability density functions show the variability of quantities at a certain instant of time. The integrated probability densities are called the probability distribution functions (PDF). These functions are plotted for the mass density and the Mach number after one large-eddy turn-over has elapsed ($t = 1.0T$). Since the flow is in the transonic regime, there is a significant variation of the mass density which is approximated by a *log-normal* distribution. In the case of the Mach number, one can see a power-law tail of the probability density towards the subsonic range ($\mathrm{Ma} \ll 1$).

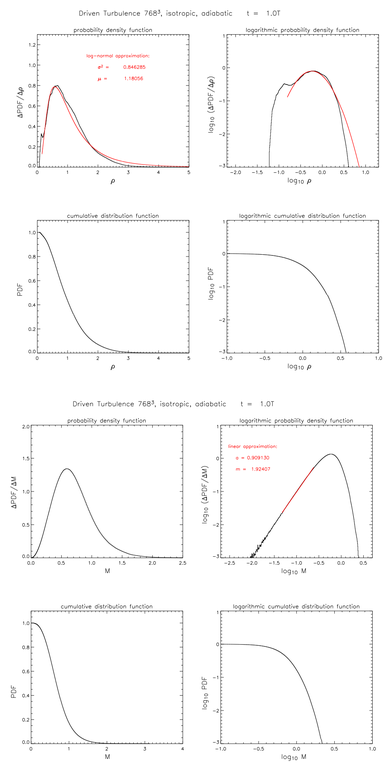

Figure 2: Probability density and distribution functions for the mass density and Mach number, respectively, both in linear and logarithmic scaling at time $t = 1.0T$.

Vorticity

- The curl of the velocity field, $\boldsymbol{\omega} = \nabla\times\boldsymbol{v}$, is called *vorticity*. High vorticity is commonly considered as the hallmark of turbulence. Probability density functions of $|\boldsymbol{\omega}|$ for consecutive instants of time are shown below. The distribution of the vorticity modulus appears to be a robust feature once the flow has reached statistical equilibrium irrespective of the gradually decreasing RMS Mach number.

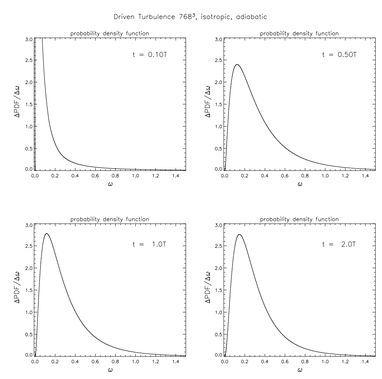

Figure 3: Probability density functions of the vorticity at different stages of the flow evolution.

- We also prepared three-dimensional visualisations of iso-surfaces of $|\boldsymbol{\omega}|$. In the early phase of flow evolution, sheet-like structures associated with shocks are forming. Subsequently, these sheets break up into smaller structures which eventually resemble the vortex filaments occurring in developed turbulence.

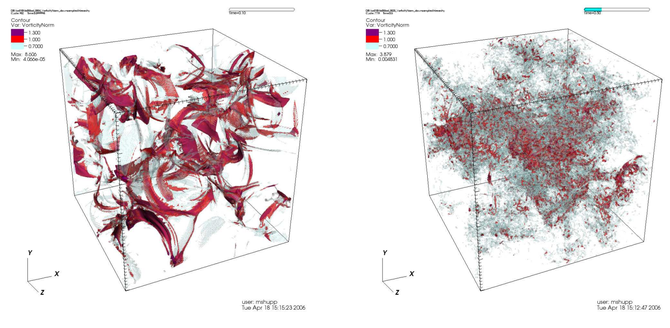

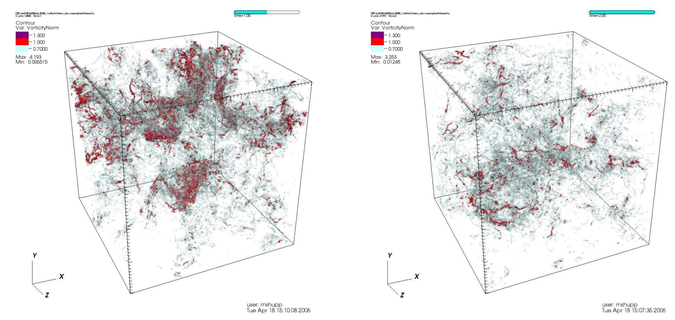

Figure 4: Visualisation of vorticity isosurfaces.

The FEARLESS Concept

- The loci of intense turbulence are found in intermittent structures such as vortex filaments or sheets aligned with shocks. For this reason, Kritsuk et al. [2006] proposed adaptive mesh refinement as an adequate numerical tool to trace these structures in the course of a simulation.
- Finding criteria that should be employed for refinement with optimal computational efficiency is a crucial problem. Intuitively, one would suspect that the numerical resolution should increase in regions subject to large strain.
- As an alternative approach, one might monitor regions in which vorticity is growing or compression increases. For example, the time evolution of the vorticity modulus in an inviscid isothermal gas is given by

$$\left(\frac{\partial}{\partial t} + \boldsymbol{v}\cdot\nabla\right) = \frac{1}{2}\left(\boldsymbol{\omega}\cdot\mathbf{S}\cdot\omega - d\omega^2\right),$$

  where $\mathbf{S}$ is the symmetric part of $\nabla\otimes\boldsymbol{v}$ and $d = \nabla\cdot\boldsymbol{v}$. The right-hand side of the above equation corresponds to the rate of vortex stretching Ξ. Vorticity is growing for $\Xi > 0$. The probability density functions of Ξ show a sharp peak at zero with a slight bias towards postive values.

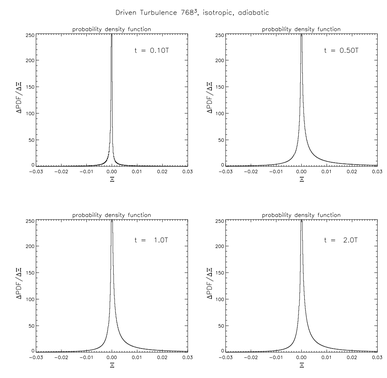

Figure 5: Probability density functions for the rate of vortex stretching.

- Based on these ideas, our goal is to implement FEARLESS (*Fluid mEchanics with Adaptively Refined Large-Eddy SimulationS*) in the Enzo code. This will also include a subgrid-scale model to treat unresolved turbulent velocity fluctuations.

References

Colella, P. and P. R. Woodward (1984). The piecewise parabolic method (PPM) for gas-dynamical simulations. *J. Comput. Physics 54*, 174–201.

Kritsuk, A. G., M. L. Norman, and P. Padoan (2006). Adaptive Mesh Refinement for Supersonic Molecular Cloud Turbulence. *Astrophys. J. Letters 638*, L25–L28.

Schmidt, W., W. Hillebrandt, and J. C. Niemeyer (2006). Numerical dissipation and the bottleneck effect in simulations of compressible isotropic turbulence. *Comp. Fluids. 35*, 353–371.